Assessing the Agility of a Variable-Tilt UAV

Joshua Taylor*, Matthew Edwards, Karl Stol, Salim Al-zubaidi, and Nicholas Kay
Department of Mechanical and Mechatronics Engineering
University of Auckland, New Zealand

ABSTRACT

Unmanned Aerial Vehicles (UAVs) have grown in popularity over recent years. However, their operation in complex environments with interference from, for example, wind and human interaction demands improved maneuverability and agility. This has brought about the rise of fully and over-actuated UAVs which can decouple translational and rotational dynamics to provide such improvements. This paper focuses on a fully-actuated variable-tilt UAV design with four rotors, all of which can be tilted collectively using two servo motors. A model of the variable-tilt UAV's horizontal thrust dynamics is presented and validated via bench-testing and flight testing of a prototype. Using this model, the key contribution of this paper is a comparison of the variable-tilt concept to an optimized fixed-tilt, over-actuated octocopter in terms of its agility, defined here as the 10-90% rise time of its horizontal thrust force response. While the octocopter currently offers greater agility, with a 70% faster rise time, the potential for improvement of the variable-tilt UAV, as well as other key benefits including improved efficiency, reduced mass, and greater suitability for UAV applications involving interaction, are explored. This provides evidence to justify continued research into variable-tilt UAVs.

1 INTRODUCTION

Unmanned Aerial Vehicles (UAVs) have experienced a rise in popularity in recent times, with applications now ranging from search and rescue to agriculture. Many of these applications require performing complex tasks in dynamic environments, often faced with disturbances such as interaction and wind field fluctuations. Typical under-actuated quadcopters, which have fewer actuators than degrees of freedom (DOFs), are often not suited to these tasks due to their coupled translational and rotational dynamics. Therefore, a need arises for UAVs with improved maneuverability and agility.

This has brought about the rise of fully-actuated and over-actuated UAVs, which have a number of actuators equal to the number of DOFs, or greater than the number of DOFs, respectively. This allows for the decoupling of DOFs such that the UAV can, for example, travel horizontally without pitching or rolling. The most common type of fully/over-actuated UAV is the fixed-tilt UAV, in which rotors (i.e., the combination of a motor and propeller) are tilted at angles to provide horizontal thrust capabilities. Research in [1] shows how an octocopter with fixed rotors tilted about the body axes improves horizontal thrust bandwidth by an order of magnitude compared to typical under-actuated UAVs. This was improved upon in [2] using a fixed-tilt UAV with a heterogeneous rotor configuration (i.e., 2 large *lift rotors*, and 6 smaller tilted *precision rotors*) which shows a further 54% increase in horizontal thrust bandwidth.

However, since the rotors of these UAVs are tilted at fixed angles and, therefore, produce opposing thrusts, they must compromise on flight endurance. This provides an opportunity to assess the performance of variable-tilt UAVs as an alternative. Variable-tilt UAVs use active tilting of the rotors during flight, typically achieved using servo motors, to provide thrust-vectoring capabilities. Control over the tilt angle allows for more efficient flight as the thrust of individual rotors can be aligned parallel to each other and in the case of hover, can be aligned directly against gravity. Variable-tilt UAVs do, however, suffer from the increased mass of the tilt actuators and the added complexity of design and control. Several variable-tilt UAV designs exist, which can be broadly categorized into independent-tilt and collective-tilt.

In independent-tilt UAVs, the orientation of each rotor can be controlled independently. Designs exist in the literature that allows for tilting in the cant angle (i.e., about an axis in line with the UAV arm) [3, 4, 5], dihedral angle (i.e., about an axis orthogonal to the UAV arm) [6, 7], as well as in both angles [8, 9]. Collective-tilt involves the simultaneous tilting of all rotors, typically via a mechanical linkage, and, therefore, usually allows for tilting in both the cant and dihedral angles [10, 11, 12]. While independent-tilt UAVs provide an element of redundancy, collective-tilting allows for fewer actuators while remaining fully-actuated, thereby benefiting from more straightforward design and control, as well as less energy expended during flight.

Assessment of the ability of these UAVs to operate in complex, dynamic environments requires a metric for agility. Several different methods have been used in the literature. In [13] a comprehensive set of 9 metrics is proposed for determining the agility of a UAV. These are determined by applying a step input during a flight test and assessing the attitude change and acceleration, for example by using the

*Email address(es): jtay996@aucklanduni.ac.nz

bandwidth based on 10–90% rise time. Alternatively, a metric is used in [1, 2], which defines agility as the horizontal thrust force bandwidth. Furthermore, in [14], agility is defined as the maximum thrust that can be produced in any direction, although this metric caters more towards omnidirectional UAVs.

In this work, a variable-tilt UAV design is explored as an alternative to fixed-tilt UAVs for complex tasks in dynamic environments. The key contribution is the use of a model of the UAV to assess its performance in terms of its agility and compare this to an existing fixed-tilt over-actuated octocopter. Another contribution is the build of a functioning prototype for validation of the model used. In Section 2, the chosen variable-tilt UAV design is described, after which the metric used to describe agility in the context of variable-tilt UAVs is covered in Section 3. Section 4 details the numerical model used for assessment of the UAV, followed by validation of the model in Section 5 and a comparison to a fixed-tilt UAV in Section 6.

2 Variable-Tilt Concept

The fully-actuated collective-tilt concept presented in [11] is chosen as a variable-tilt UAV to assess. This is shown in Figure 1, where f_{Pi} and m_{Pi} are the thrust force and moment produced by the ith rotor, and body-fixed axes are defined at the center of the upper structure. This design uses a 2-DOF actuated joint at the center of the UAV, which collectively drives four rotors using a mechanism consisting of four four-bar linkages. All joints, excluding the actuated joint, provide three rotational DOFs to allow for tilting of the rotors in any direction.

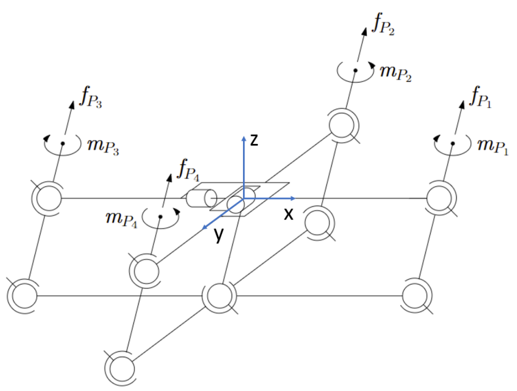

Figure 1: The variable-tilt concept presented in [11] assessed in this work

The coordinate system used to describe rotor orientation is shown in Figure 2, where θ is referred to as the tilt angle, and ϕ as the azimuth. Given that the four-bar linkages that drive the tilting of the rotors form parallelograms, the orientation of each rotor and the center linkage is identical and can be described by one shared tilt angle and azimuth.

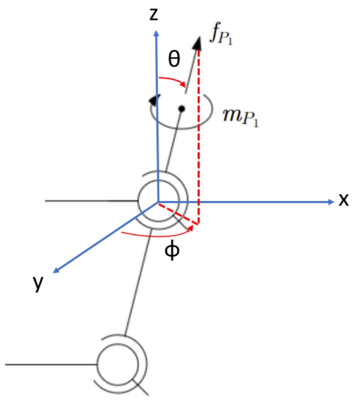

Figure 2: The coordinate system used to describe the orientation of the rotors

3 Agility

As described in [13], there are various approaches to measuring agility, but no standard for multi-rotors. The metric chosen in this paper is the 10-90% rise time of horizontal thrust to a step input. This measure allows for non-linearities such as those introduced by the saturation of servo motors typically used for tilting.

More specifically, agility will be measured from the open-loop response of the UAV to a step input that drives a transition from zero horizontal thrust to maximum horizontal thrust. In the case of the variable-tilt UAV, this will involve a step input to the tilt actuators and a simultaneous voltage step input to the rotors in order to maintain vertical equilibrium.

4 Numerical Model

A model of the variable-tilt UAVs ability to produce horizontal thrust is presented to measure its response to the step input described in Section 3. The characteristics of the horizontal thrust response are assumed to be dependent purely on the dynamics of the rotors and the tilting actuators; therefore, the model comprises these parts. While geometric coupling between the rotor and servo motor is considered in the model, the effects of dynamic coupling, for example, the effect of the spinning rotor on the tilting actuator load as it passes through the air during tilting, is assumed to be negligible. Additionally, the model assumes that no latency is introduced into the system by electronic components.

The thrust, T, in N produced by each rotor is modeled as a function of its rotational velocity, ω, in rad/s as per:

$$T = c_T\omega^2 \tag{1}$$

where c_T is the thrust constant.

The direction of thrust relative to the body axis (i.e., the tilt angle) is determined by the tilting actuators' response to the step input. Given that servo motors are used, this is considered to be dominated by saturation and the response is, therefore, modeled by a rate limit, as per:

$$\dot{\theta} = \begin{cases} \dot{\theta}_{ref} & \text{if } \dot{\theta}_{ref} < \dot{\theta}_{max} \\ \dot{\theta}_{max} & \text{if } \dot{\theta}_{ref} \geq \dot{\theta}_{max} \end{cases} \tag{2}$$

where $\dot{\theta}$ is the rotational velocity of the tilt servo in rad/s, $\dot{\theta}_{ref}$ is the reference rotational velocity, and $\dot{\theta}_{max}$ is the rate limit.

To maintain vertical equilibrium during the step response, the following constraint is applied on the UAV throughout:

$$4Tcos(\theta) = mg \tag{3}$$

where m is the mass of the UAV in kg, and g is gravity acceleration in m/s^2.

Changes in rotor speed are required to satisfy this constraint, as per (1), and the speed dynamics of each rotor are modeled using the non-linear equation of motion presented in [15]:

$$J_{rotor}\dot{\omega}_i = \frac{V_0 - I_0 R}{R K_V V_0}\left(V - I_0 R - \frac{V_0 - I_0 R}{K_V V_0}\omega_i\right) - c_\tau {\omega_i}^2 \tag{4}$$

where J_{rotor} is the inertia of the rotor in kgm^2, $\dot{\omega}_i$ is the rotational acceleration of the ith rotor in rad/s^2, V_0 is the motor's nominal Voltage in V, I_0 is the idle current in mA, R is the motor resistance in Ω, K_V is the motor speed constant in $rad/s/V$, and c_τ is the torque constant in Nms/rad.

5 Validation of the Model

To validate the model of the variable-tilt UAV's horizontal thrust dynamics, a physical prototype of the variable-tilt concept was built for bench and flight testing. Bench-testing allowed for more accurate sensor data when measuring the force response and was used to validate the model across a range of parameter changes, including changes to flying mass, tilt angle, and azimuth. The flight test validates the bench-test data, as well as the expected flight dynamics of decoupled DOFs.

5.1 Prototype

The prototype developed is shown in Figure 3. The sheet components of the main body and arms are made from cut carbon fiber or acrylic, and the remaining components are primarily designed as 3D-printed parts. The joints are realized using bearings to allow for rotation while still maintaining rigidity in the arms. To assess the capabilities of the UAV, only tilting in on-axis azimuths (i.e., 0°, 90°, 180°, and 270°) is tested, and therefore the use of 2-DOF joints for the four-bar linkages is sufficient. The key components used in the UAV prototype are listed in Table 1.

The model parameters corresponding to the UAV prototype using these components are listed in Table 2. J_{rotor} was determined by modeling the propeller as a slender rigid rod, and c_τ and c_T were determined empirically by fitting curves to torque-speed and thrust-speed data, respectively, obtained using a load cell. The servo rate limit was obtained experimentally from the saturated region of a step response measured using feedback from a DYNAMIXEL MX-28T servo under no load. Testing under several different loading conditions that might be experienced by the servo motor showed negligible change in the rate limit measured. The remaining model parameters were taken from component specifications provided by the manufacturers.

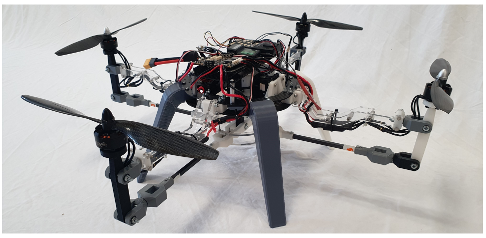

Figure 3: The prototype variable-tilt UAV developed for validation

Component	Product
Flight Controller	Pixhawk 4
Motors	RCTIMER MT2610-920KV
Propellers	10×4.7”
Electronic Speed Controllers (ESC)	RCTIMER NFS 30 A
Battery	4S 2500mAh
Tilt Servo	Dynamixel MX-28T

Table 1: Key components used in variable-tilt UAV prototype

Parameter	Value
J_{rotor}	5.3763×10^{-5}
c_T	1.976×10^{-5}
c_τ	3.956×10^{-7}
V_0	$16\,V$
Kv	$93.64\,rad/s/V$
I_0	$0.7\,A$
I_{max}	$30\,A$
R	$0.11\,\Omega$
$\dot{\theta}_{max}$	$5.41\,rad/s$

Table 2: Model Parameters for UAV Prototype

The characteristics of the prototype variable-tilt UAV are listed in Table 3. Note that the maximum horizontal thrust can be limited by the maximum allowable tilt angle of the frame, or by the maximum thrust that can be produced by the rotors themselves. In the case of this prototype, the limiting factor is the frame, which can tilt up to 15°.

Characteristic	Value
Expected Maximum Horizontal Thrust ($\theta = 15°$)	7.97 N
Payload	1 kg
Expected Hover Endurance	5 min
Flying Mass	3 kg
UAV Radius	300 mm

Table 3: Characteristics of the prototype variable-tilt UAV

5.2 Bench-test

5.2.1 Setup

Bench-testing involved fixing the prototype to a JR3 6DOF force balance as shown in Figure 4. Since the tilting mechanism is located on the underside of the UAV, to allow for a simple connection to the force balance, it was mounted upside-down. As the UAV was raised from the ground, the mounting orientation was considered to have a negligible effect on the rotor aerodynamics. The force balance has a resolution of 0.005 N and an upper limit of 40 N in the horizontal plane, and samples were acquired at 1000 Hz via a data acquisition card. To allow for long periods of testing with consistent voltages, a power supply was used instead of batteries.

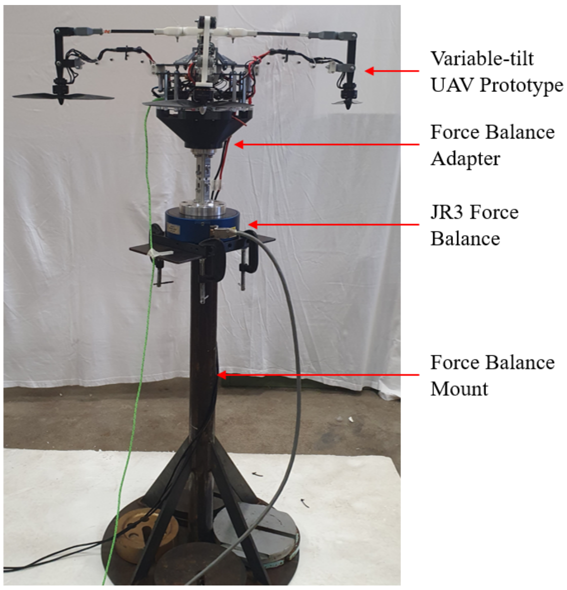

Figure 4: Bench-test setup for the variable-tilt UAV prototype

To apply the required step inputs to measure agility, the pulse width modulation (PWM) signal sent to the ESCs was controlled directly, bypassing any control schemes typically used by the flight controller. Given the flying mass of the UAV that is being tested and the equilibrium condition (3), the hover thrust that needs to be produced via the rotors is known, and using (1) can be used to determine the necessary rotational speed of the rotors. Using (4) at steady-state (i.e., $\dot{\omega} = 0$) then relates V to this required ω, thereby defining the reference voltage values before and after a horizontal thrust is produced. The duty cycle, D, of the corresponding PWM signal used to control the rotor voltage can be determined by:

$$V = DV_0 \tag{5}$$

where D then translates to a 1-2ms pulse sent to the ESCs.

5.2.2 Signal Processing

Due to the low signal-to-noise ratio (SNR) of the data collected by the force balance, as can be seen in Figure 5, the data is processed before analysis. A significant portion of this noise can be linked to vibration caused by rotor asymmetry. Testing of individual rotors showed that resonance is reached near the range of hover conditions tested during bench-testing (i.e., 1400-1500 μs) as shown in Figure 6.

Given that filtering has the effect of smoothing a response, it is crucial that an appropriate filter is used, and that the time resolution is maintained while minimizing the noise. A third-order low-pass elliptic filter with a cutoff frequency of 20 Hz is chosen. A forward and backward pass of the filter over the data is performed, thereby effectively increasing the order of the filter to sixth-order and ensuring zero phase distortion is introduced. The filtered data is also shown for the sample presented in Figure 5.

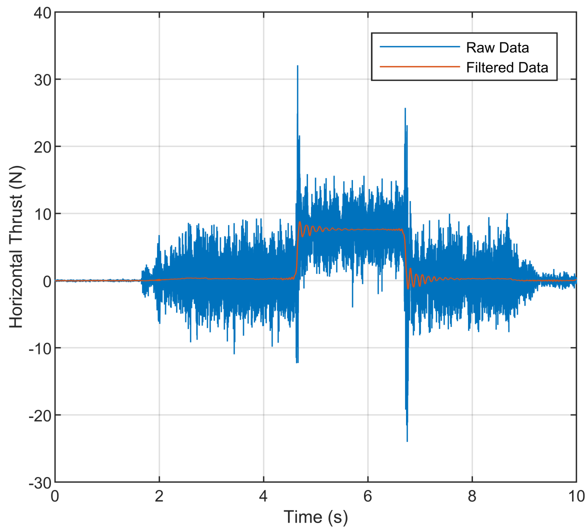

Figure 5: Data measured by the JR3 force balance (flying mass = 3 kg, $\theta = 15°$, $\phi = 0°$)

5.2.3 Results

The first test case corresponds to a flying mass of 3 kg, a final tilt angle of 15°, and an azimuth of 0°, such that an expected final horizontal thrust of 7.97 N is produced. The step response is shown in Figure 7, alongside the corresponding

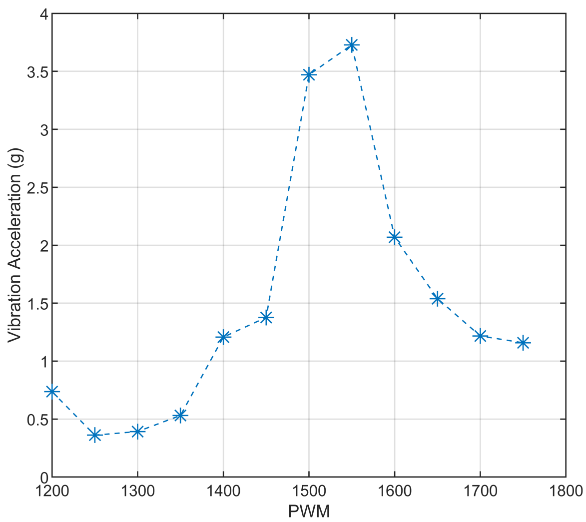

Figure 6: Vibration of the rotor at different PWM signals

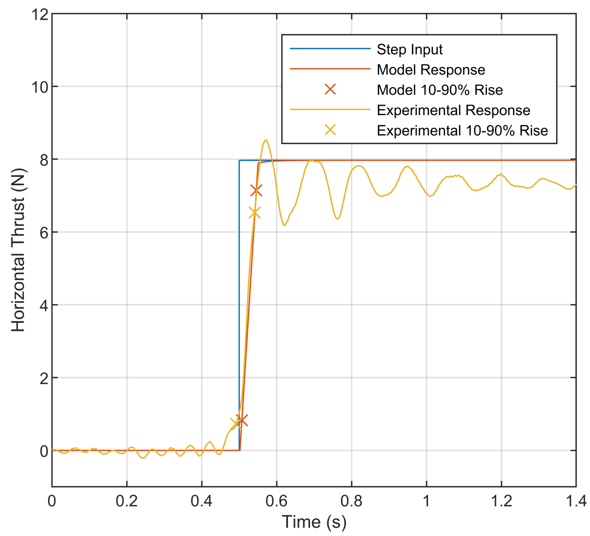

Figure 7: Comparison between the model response and experimental response (flying mass $= 3\,\text{kg}$, $\theta = 15°$, $\phi = 0°$)

response produced by the model. The response shows significant overshoot and oscillation, however, high-speed camera footage of the tilting confirmed that this was a component of the actual response, and not a consequence of filtering. Fortunately, 10-90% rise time as a measure of agility is robust to this, as it does not consider steady-state oscillations to the same extent as a measure such as settling time might.

It is clear from Figure 7 that there is a small amount of error at steady state. This could be the result of imperfections in the frame's geometry leading to inaccurate thrust vectoring or its vibration leading to a reduction in the efficiency of the rotors and, therefore, c_T which was measured for the model by fixing the rotor to a more rigid mount. However, despite the need for improvement in the rotor model, the gradient during saturation is very similar between the model response and the experimental response. Across 8 measured time responses for these testing parameters, a mean 10-90% rise time for the experimental data of 49.7 ms was recorded, which is very similar to the 38.6 ms rise time produced by the model. This provides a foundation for validating the model for the purposes of providing an accurate measure of agility. It is likely that considering the behavior of the servo motor outside the region of saturation would increase the rise time produced by the model, thereby somewhat resolving the small difference between the numerical and experimental data. Additionally, although minimal, residual effects from the filtering are likely to increase experimental rise time slightly, which might further explain the difference to the model.

Given that the rise times measured could vary due to different loading for the two tilt actuators and varying friction in the joints, testing was completed for a tilt angle of 15° along all other on-axis azimuths (i.e., ϕ = 90°, 180°, and 270°). This was repeated 8 times. The measured rise times are shown in Figure 8, which demonstrates that, while there are subtle differences present, for the most part, they remain approximately consistent in all four primary directions, providing further confidence in the model.

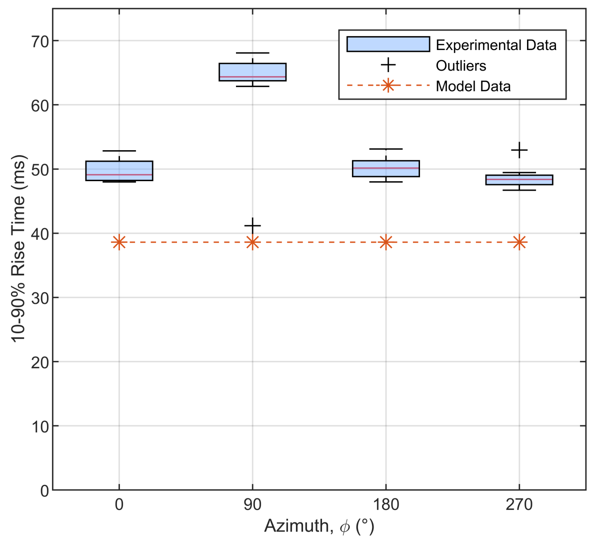

Figure 8: Rise times at different azimuths (flying mass $=$ $3\,\text{kg}$, $\theta = 15°$)

To further validate the model, as well as how well it scales to different parameter changes, bench-testing was conducted for step inputs of a 15° tilt angle at an azimuth of 0° for different hover thrust conditions. PWM values of $1400\,\mu s$, $1450\,\mu s$, and $1500\,\mu s$ were tested which correspond to the hover conditions for flying masses of 2.07 kg, 2.54 kg, and 3.00 kg, respectively. The rise times are shown in Figure 9. Once again, while the rise times are similar, there are slight differences which further suggest that there is a component of the system that is being misrepresented or ignored in the model. However, the model data appears to accurately capture the trend of the experimental data. This relatively constant trend can also be expected given that the only difference when changing the hover PWM lies in the rotor dynamics, which, as a first-order system, will not change significantly.

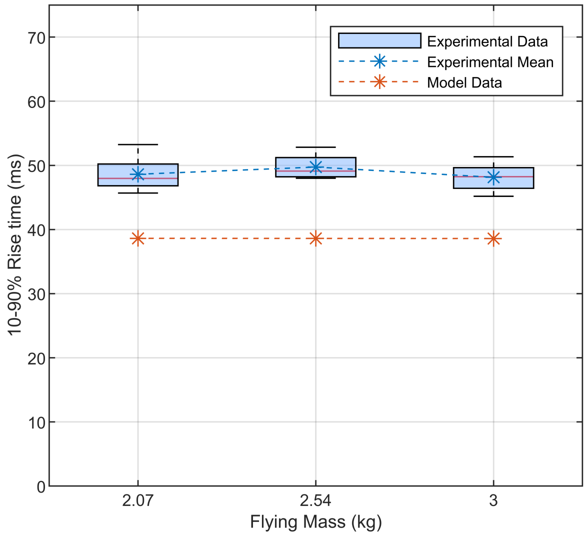

Figure 9: Rise times at different flying masses ($\theta = 15°$, $\phi = 0°$)

Finally, the trend observed when adjusting the tilt angle of the UAV for a 3 kg flying mass and azimuth of 0° was tested and compared, as shown in Figure 10. As with previous testing, there is a slight difference in rise times between the experimental and model data, however, the trend remains approximately the same. In both cases, a rising trend in 10-90% rise time can be seen as the tilt angle increases. Interestingly, as the tilt angle increases, the model data appears to more accurately represent the actual system. This is likely because, for greater tilt angles, there is a larger saturated portion of the response relative to the response as a whole. Therefore, at larger tilt angles, the system more closely resembles the model when dominated by a rate limit.

Overall, while there exist some differences between the 10-90% rise time values produced by the model and experimental data, the model is reasonably validated, in particular for larger tilt angles and for the purposes of analyzing trends produced by varying model input parameters.

5.3 Flight Tests

5.3.1 Setup

A step input was applied to the tilting actuators from 0° to 15°, and a 1 kg payload was mounted to the UAV (i.e., a flying mass of 3 kg), to replicate the test shown in Figure 7. The rotor throttle was adjusted throughout flight to maintain vertical equilibrium, however, this was performed manually and, therefore, the results presented for flight tests are indicative

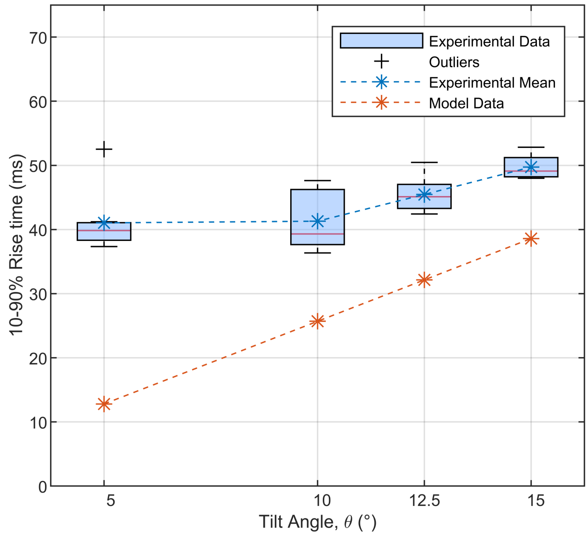

Figure 10: Rise times at different tilt angles (flying mass = 3 kg, $\phi = 0°$)

only. The position of the UAV was recorded during flight with millimeter accuracy using a Vicon motion capture system. The second derivative of this position data gives the acceleration response, of which the measured rise time corresponds to the rise time of the horizontal thrust force response.

5.3.2 Results

Observation of the UAV's flight validates its ability to decouple DOFs. The UAV traveled horizontally due to tilted rotors, while the main body of the UAV remained level with the ground. This is demonstrated in Figure 11, which shows less than 1° of rotation about the pitch axis during horizontal flight. Although it is minor, the UAV pitch angle experienced a sudden drop and recovery as the step input was initially applied, which is likely due to the momentum of the tilting structure, as well as the minor change in center of mass, which had to be accounted for by the pitch controller.

A comparison of the rise time measured from the acceleration response shown in Figure 11 with that measured from the equivalent bench-test validates the accuracy of the data collected from the bench-testing set-up. For a 3 kg flying mass and a final tilt angle of 15° in the 0° azimuth, the bench-test yielded a mean rise time of 49.7 ms, whereas the flight test produced a slightly higher value of 60.1 ms. Since the flight test accounts for all of the UAV's dynamics, instead of isolating the tilting mechanism itself as in the bench-test, there exists a slight difference in these values. Note that this difference is likely magnified by errors introduced by manual control during flight, as the UAV's altitude increased by 233 mm over the time sample shown in Figure 11. However, given that the flight test rise time is in the same order of magnitude as that measured via equivalent bench-testing, this pro-

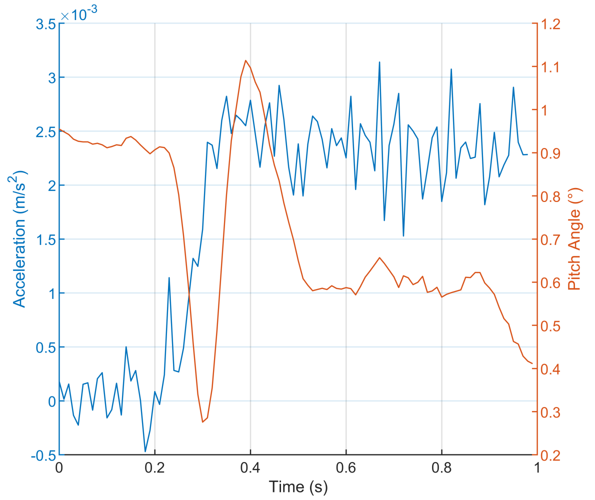

Figure 11: Horizontal acceleration and pitch angle during step-input (flying mass $= 3\,\text{kg}$, $\theta = 15°$)

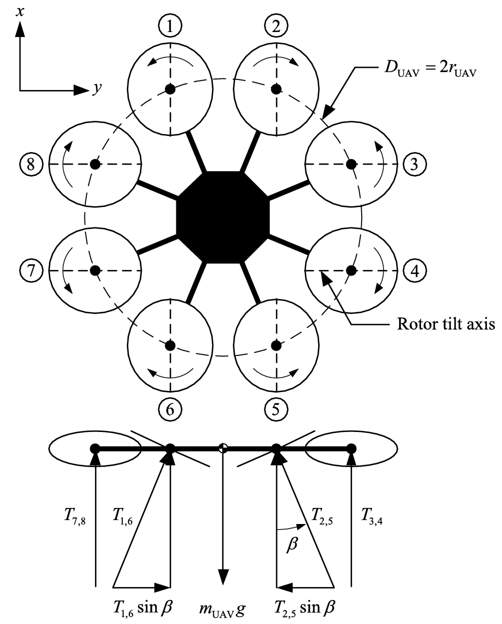

Figure 12: Fixed-tilt over-actuated octocopter [16]

vides further confidence in the bench-test data.

6 COMPARISON TO A FIXED-TILT UAV

To assess how effective the variable-tilt platform is as a method of achieving fully-actuated flight, a comparison is drawn to an existing fixed-tilt, over-actuated octocopter [1, 16]. This UAV is shown in Figure 12 where D_{UAV} is the UAV's diameter, r_{UAV} is the radius, T is the thrust, and β is the common tilt angle about the body (i.e., orthogonal) axes.

In this comparison, the agility of both UAVs is assessed using numerical models. As well as the model of the variable-tilt UAV's horizontal thrust dynamics having been validated, use of this for comparison is deemed acceptable given that the numerical model of the fixed-tilt UAV uses the same equations to describe rotor dynamics [16].

In [16], a parameter sweep is used to generate the parameters and performance characteristics of an optimized octocopter. This draws from a collection of rotors and a range of tilt angles and airframe diameters to find the best octocopter configuration that satisfies three constraints: a specified payload, minimum flight time, and minimum level of horizontal thrust. In this case, these constraints are defined by the variable-tilt UAVs characteristics from Table 3 as 1 kg, 5 min, and 7.97 N, respectively. Table 4 provides a comparison between the resultant octocopter and the variable-tilt UAV.

While the octocopter outperforms the variable-tilt UAV in terms of agility, it is important to consider that the comparison is made between an unoptimized variable-tilt UAV and an optimized fixed-tilt UAV. Since the rise time values between the two UAVs are within the same order of magnitude, this indicates potential for the variable-tilt UAV. A simple parameter sweep that takes in a range of servo motors with higher rate limits could offer improvements to rise time.

Furthermore, it is interesting to note that the variable-tilt UAV achieves similar flight characteristics and performance at a lower flying mass. A key contributing factor here is the battery mass. The required battery mass of the fixed-tilt UAV to achieve the set flight time and payload is 868 g, whereas the variable-tilt UAV only requires a 212 g battery. This is due to the improved flight efficiency, as the rotors can produce direct vertical thrust during hover. This, therefore, addresses one of the key limitations of fixed-tilt fully/over-actuated UAVs discussed in the literature.

Characteristic	**Variable-tilt UAV**	**Fixed-tilt UAV**
Flying Mass	3 kg	3.41 kg
UAV Radius	300 mm	300 mm
Maximum Horizontal Thrust	7.97 N	8.43 N
Flight Time	5 min	5 min
Agility (10-90% rise time)	38.6 ms	11.6 ms
Adjacent Rotor Clearance	170 mm	157 mm

Table 4: Comparison between the variable-tilt design and the fixed-tilt design

Another consideration to be made when comparing the two designs relates to the applications of the UAVs themselves. Given that it is often desirable to fit a manipulator to the front of a UAV, it is beneficial to have greater clearance between adjacent rotor tips, which the variable-tilt UAV has.

7 CONCLUSION

This paper assesses a variable-tilt, fully-actuated quadcopter as an alternative to a fixed-tilt, over-actuated octocopter for use in applications where the UAV must deal with complex disturbances such as wind-field fluctuations and interaction. Performance is measured in terms of the UAV's agility, defined as the 10-90% rise time of the open-loop horizontal thrust response. A validated model was developed to measure the agility of the variable-tilt UAV and this was used to conduct the comparison to the octocopter. While the rise time is shorter for the fixed-tilt UAV, given that an unoptimized variable-tilt UAV produced results within the same order of magnitude and benefits from improved efficiency, there is reason to continue research in the area of variable-tilt UAVs for applications in dynamic environments.

Future work will involve further improvements to the model such that it can be used in an optimization of the design of the variable-tilt UAV. This will allow for an improved comparison between the variable-tilt and fixed-tilt UAVs. Following this, the study would benefit from further verification via flight testing. To provide horizontal thrust in all directions (i.e., all azimuths), 3-DOF joints will be added to the UAV.

ACKNOWLEDGEMENTS

The research reported in this article was conducted as part of “Enabling unmanned aerial vehicles (UAVs) to use tools in complex dynamic environments UOCX2104”, which is funded by the New Zealand Ministry of Business, Innovation and Employment.

REFERENCES

[1] Z Jeremy Chen, Jérémie XJ Bannwarth, Karl A Stol, and Peter J Richards. Analysis of a multirotor uav with tilted-rotors for the purposes of disturbance rejection. In *2018 International Conference on Unmanned Aircraft Systems (ICUAS)*, pages 864–873. IEEE, 2018.

[2] Salim Al-Zubaidi and Karl A Stol. Preliminary design optimisation of a novel fixed-tilt heterogeneous uav for horizontal agility. In *2022 International Conference on Unmanned Aircraft Systems (ICUAS)*, pages 1489–1496. IEEE, 2022.

[3] Alireza Nemati and Manish Kumar. Modeling and control of a single axis tilting quadcopter. In *2014 American Control Conference*, pages 3077–3082. IEEE, 2014.

[4] Markus Ryll, Heinrich H Bülthoff, and Paolo Robuffo Giordano. A novel overactuated quadrotor unmanned aerial vehicle: Modeling, control, and experimental validation. *IEEE Transactions on Control Systems Technology*, 23(2):540–556, 2014.

[5] Mina Kamel, Sebastian Verling, Omar Elkhatib, Christian Sprecher, Paula Wulkop, Zachary Taylor, Roland Siegwart, and Igor Gilitschenski. The voliro omniorientational hexacopter: An agile and maneuverable tiltable-rotor aerial vehicle. *IEEE Robotics & Automation Magazine*, 25(4):34–44, 2018.

[6] Sherif Badr, Omar Mehrez, and AE Kabeel. A novel modification for a quadrotor design. In *2016 International Conference on Unmanned Aircraft Systems (ICUAS)*, pages 702–710. IEEE, 2016.

[7] Mohammadhosein HajiAbedini, Fatemeh Zargarbashi, Amin Talaeizadeh, Hossein Nejat Pishkenari, and Aria Alasty. Design and implementation of a novel overactuated quadrotor with variable dihedral angle. In *2021 9th RSI International Conference on Robotics and Mechatronics (ICRoM)*, pages 391–398. IEEE, 2021.

[8] Ali Bin Junaid, Alejandro Diaz De Cerio Sanchez, Javier Betancor Bosch, Nikolaos Vitzilaios, and Yahya Zweiri. Design and implementation of a dual-axis tilting quadcopter. *Robotics*, 7(4):65, 2018.

[9] Pau Segui-Gasco, Yazan Al-Rihani, Hyo-Sang Shin, and Al Savvaris. A novel actuation concept for a multi rotor uav. *Journal of Intelligent & Robotic Systems*, 74(1):173–191, 2014.

[10] Peter Zheng, Xinkai Tan, Basaran Bahadir Kocer, Erdeng Yang, and Mirko Kovac. Tiltdrone: A fully-actuated tilting quadrotor platform. *IEEE Robotics and Automation Letters*, 5(4):6845–6852, 2020.

[11] Marcin Odelga, Paolo Stegagno, and Heinrich H Bülthoff. A fully actuated quadrotor uav with a propeller tilting mechanism: Modeling and control. In *2016 IEEE international conference on advanced intelligent mechatronics (AIM)*, pages 306–311. IEEE, 2016.

[12] Michelangelo Nigro, Francesco Pierri, and Fabrizio Caccavale. Preliminary design, modeling and control of a fully actuated quadrotor uav. In *2019 International Conference on Unmanned Aircraft Systems (ICUAS)*, pages 1108–1116. IEEE, 2019.

[13] Jon Verbeke and Joris De Schutter. Experimental maneuverability and agility quantification for rotary unmanned aerial vehicle. *International Journal of Micro Air Vehicles*, 10(1):3–11, 2018.

[14] Dario Brescianini and Raffaello D'Andrea. An omnidirectional multirotor vehicle. *Mechatronics*, 55:76–93, 2018.

[15] Dongjie Shi, Xunhua Dai, Xiaowei Zhang, and Quan Quan. A practical performance evaluation method for electric multicopters. *IEEE/ASME Transactions on Mechatronics*, 22(3):1337–1348, 2017.

[16] ZJ Chen, KA Stol, and PJ Richards. Preliminary design of multirotor uavs with tilted-rotors for improved disturbance rejection capability. *Aerospace Science and Technology*, 92:635–643, 2019.